FERMILAB-PUB-20-596-E-V
ACCEPTED

Prepared for submission to JINST

An approach to light distribution for the calibration of high energy physics calorimeters

A. Anastasi[a,1], **E. Bottalico**[a,c], **G. Cantatore**[d,e], **L. Cotrozzi**[a,c], **S. Dabagov**[h,i,j], **R. Di Stefano**[b,l], **A. Driutti**[d,f], **C. Ferrari**[a,m], **A. Fioretti**[a,m], **C. Gabbanini**[a,m], **M.D. Galati**[a,c], **A. Gioiosa**[k,o], **P. Girotti**[a,c], **D. Hampai**[h], **M. Iacovacci**[b,q], **M. Incagli**[a], **M. Karuza**[d,q,2], **A. Lusiani**[a,n], **F. Marignetti**[b,l], **S. Mastroianni**[b], **A. Nath**[b], **G.M. Piacentino**[k,o], **N. Raha**[a], **L. Santi**[d,f], **M. Sorbara**[k,g], **G. Venanzoni**[a], **V. Vujnović**[q]

[a] *INFN, Sezione di Pisa, Largo Bruno Pontecorvo 3, I-56127 Pisa, Italy*

[b] *INFN, Sezione di Napoli, Complesso Universitario di Monte Sant'Angelo, via Cinthia, I-80126 Napoli, Italy*

[c] *Dipartimento di Fisica, Università di Pisa, Largo Bruno Pontecorvo 3, I-56127 Pisa, Italy*

[d] *INFN, Sezione di Trieste, via A. Valerio 2, I-34127 Trieste, Italy*

[e] *Dipartimento di Fisica, Università di Trieste, via A. Valerio 2, I-34127 Trieste, Italy*

[f] *INFN, G.C. di Udine e Università degli Studi di Udine, Via delle Scienze 208, I-33100 Udine, Italy*

[g] *Dipartimento di Fisica dell'Università di Roma Tor Vergata, via della Ricerca Scientifica 1, I-00133 Roma, Italy*

[h] *Laboratori Nazionali di Frascati dell'INFN, Via Enrico Fermi 40, I-00044 Frascati, Italy*

[i] *P.N. Lebedev Physical Institute RAS, Leninsky Ave. 53, 119991 Moscow, Russia*

[j] *National Research Nuclear University "MEPhI", Kashirskoe Str. 31, 115409 Moscow, Russia*

[k] *INFN, Sezione di Roma Tor Vergata, via della Ricerca Scientifica 1, I-00133 Roma, Italy*

[l] *Università di Cassino, Via G. Di Biasio 43, I-03043 Cassino, Italy*

[m] *Istituto Nazionale di Ottica, CNR-INO, S.S. 'A Gozzini', via G. Moruzzi 1, I-56124 Pisa, Italy*

[n] *Scuola Normale Superiore, Piazza dei Cavalieri 7, I-56126 Pisa, Italy*

[o] *Università degli studi del Molise, Dipartimento Bioscienze e Territorio, Contrada Fonte Lappone, I-86090 Pesche, Italy*

[p] *Dipartimento di Fisica, Università di Napoli "Federico II", Complesso Universitario di Monte Sant'Angelo, via Cinthia, I-80126 Napoli, Italy*

[q] *Department of Physics and Centre for Micro Nano Sciences and Technologies, University of Rijeka, Radmile Matejcic 2, 51000 Rijeka, Croatia*

E-mail: mkaruza@uniri.hr

[1] Deceased

[2] Corresponding author

Abstract:

In high energy physics experiments, calorimeters are calibrated to produce precise and accurate results. Laser light can be used for calibration when the detectors are sensitive to photons in that particular energy range, which is often the case. Moreover, it is not unusual that detection systems consist of hundreds of channels that have to be calibrated independently, which produce stringent requirements on the light distribution system in terms of temporal and spatial stability, energy distribution and timing. Furthermore, the economic factor and the ease of production have to be taken into account. We present a prototype light distribution system, based on a series of optical beamsplitters, developed for the Muon g-2 experiment at Fermilab.

Keywords: calibration, light distribution, laser

Contents

1 Introduction **1**

2 Front panel design **3**
2.1 Output beam matrix photon statistics 5

3 Front panel tests **7**
3.1 Alignment precision and mechanical stability 7
3.2 Light distribution 8
3.3 Light diffusion 10

4 Conclusion **12**

1 Introduction

The complexity of the detectors in high energy physics is growing over time due to the increasing size and segmentation of detectors, which increases the number of channels needed to provide details about the position of the signal and to avoid its pileup. Furthermore, accurate information regarding the amplitude of the signal is required, which is only achievable by the continuous calibration of each channel [1–4]. Thus a complex calibration system has to be built. The complexity of the systems is sometimes increased by geometrical constraints imposed by the experimental setup which is the case of the Muon g-2 experiment.

The Muon g-2 experiment presently running at Fermi National Accelerator Laboratory (FNAL) in the United States of America has been constructed with the goal of improving the previous results of the measurement of the anomalous magnetic moment of the muon [5]. The previous results show a $> 3\sigma$ discrepancy between the measurement and theoretical prediction. This discrepancy is difficult to accommodate within the Standard Model (SM) and more precise measurements are needed. In case the previous results are confirmed, this would be a possible indication of the existence of new physics beyond the SM. The Muon g-2 experiment uses the muon storage ring from the Brookhaven E-821 experiment, [6] which has been shipped to FNAL and installed in a new dedicated building. The polarized muons arriving from the FNAL accelerator are stored in the ring for 700 μs before they decay into positrons. Due to the parity violation in weak interaction, the high energy positrons are preferentially emitted in the direction of the muon spin. They are detected in a series of calorimeters (24) equally distributed around the ring (see Fig.1). Each calorimeter consists of 54 PbF_2 [7] crystals where Cherenkov light created by incoming positrons is detected by one detector for each crystal. This totals to almost 1300 channels that have to be simultaneously monitored and calibrated.

In the case the measured quantity is given by a pulse of light, a laser pulse of similar characteristics can be used for the detector calibration. This includes Cherenkov radiation and scintillation

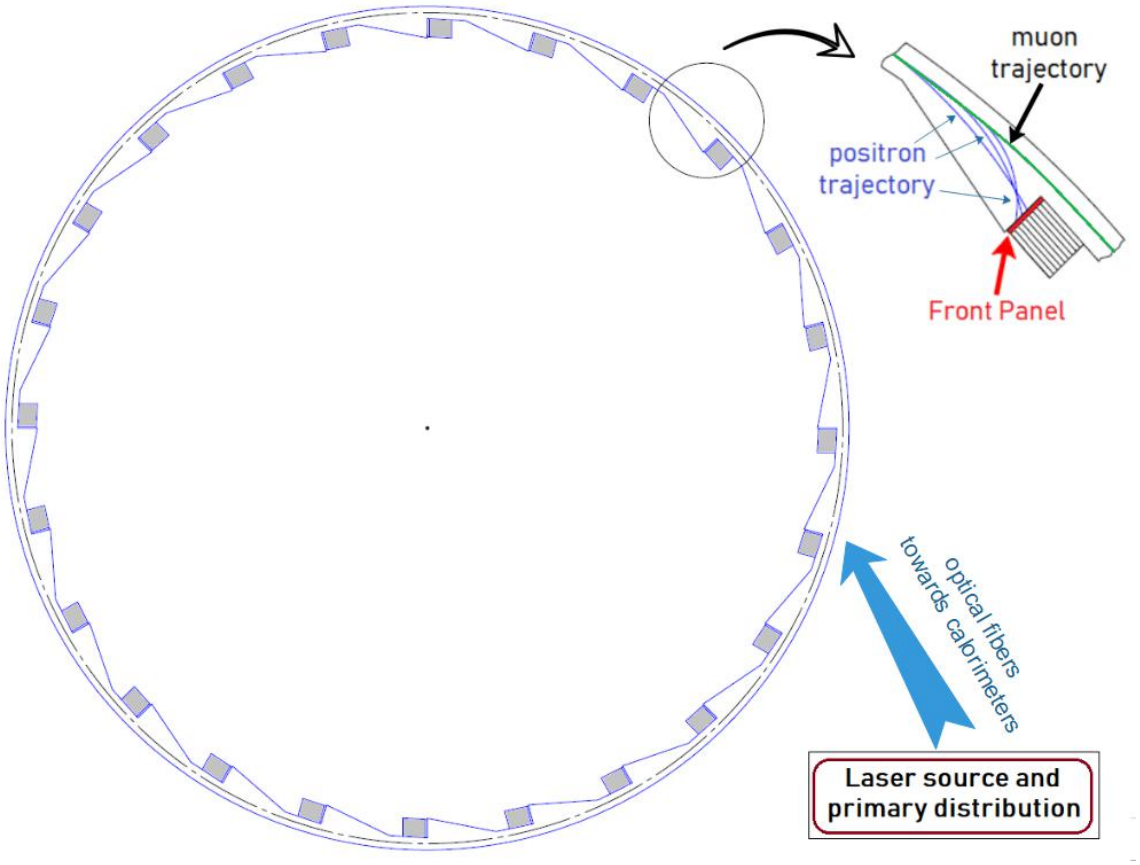

Figure 1. A scheme of the Muon g-2 storage ring. The 24 calorimeters are distrubuted around the ring. In the exploded view a calorimeter station is shown with the position of the front panel. The laser source and primary distribution are positioned outside the ring.

processes. An additional challenge, besides the mechanical constraints, lies in providing an identical calibration signal for each and every channel of the detector system. The number of channels varies from experiment to the experiment, but it can easily reach into the thousands [1]. The obvious solutions for providing a calibration signal include illuminating each of the channels with a dedicated light source, or dividing the light coming from one source to an adequate number of channels. One potential limitation of the first approach is that it requires an independent light source and corresponding monitor for each channel.

The monitoring is necessary to guarantee the stability in amplitude and shape of the calibration pulse sent to the detectors. An example is provided by the monitoring light distribution system in the CMS experiment where the system receives laser pulses from the fibre optic switch at the source and injects them into individual crystals via a three-level optical fibre distribution system [2]. In the second approach, the number of monitors is reduced to one, but the division of an intense light pulse into thousands of less intense pulses can become quite complicated [3]. The distribution system has to provide equal light intensity for every channel while maintaining consistency over time [4]. To achieve these requirements at the detectors, a large amount of light is often lost. The use of integrating spheres is a prominent example of this effect. This method also involves the

use of intense light sources which create safety, budget and other issues. A dedicated calibration system was constructed for Muon g-2 experiment [8] while here we present an alternative approach where the distribution system is constructed from a series of custom made beamsplitters. The requirements on the detector side of the experiment are $\frac{\delta G}{G} < 1\%$ in terms of gain change during few seconds, while $\frac{\delta G}{G} < 0.1\%$ is required for the duration of muon fill, i.e. in a fraction of second. The fluctuations of the laser pulse intensity should be lower than the accepted gain changes in order to be able to correct for eventual variations. The requirement on the energy resolution is less stringent, up to 5%, hence the differences in delivered light intensities to different channels up to few percent could be accepted. The performance of the distribution system in terms of channel equalisation and stability is given.

2 Front panel design

In order to distribute the light to 54 channels that are present in each of the calorimeters a light distribution element called front panel was designed. The main idea and constraint came from the space available (2−3 cm) in the Muon g-2 experiment between the vacuum chamber and the detector station. In this space, a light source has to be inserted for the calibration. This can be done in various ways. For example, a light source can be inserted in front of the crystals, or light coming from a remote source can be carried by optical fibres to the sensor station. Unfortunately, the available space is too tight for most of the optical fibres to make a 90° bend. Considering the light source, geometry, and monitoring needs of the Muon g-2 experiment, fibres would need to guide light in the near UV and visible spectra and have a bend radius less than 2 cm. Commercially available multimode fibres from both Newport and Thorlabs exist that satisfy the radius requirement. However, limited core diameter, bend losses, and complicated production makes this solution impractical. In addition, while bending losses can be calculated theoretically using formula derived by Sakai and Kimura [9], the absolute value of the bend losses is difficult to interpret since measurements on longer bent lengths revealed a strong dependence of the bend loss at a particular point on the geometry of the fibre layout preceding that point. Most notably, a large decrease in bend loss after a sufficient length in fibre was observed, as well as a dependence of the bend loss on the straight segment between bends [10]. In order to avoid surpassing the bend radius limit, an alternative solution has to be found. For example steering mirrors or reflecting prisms between the front of the detector and fibre output can be placed in order to deviate the light by 90° [11]. While solving the possible problems arising from the bending of fibres, this solution complicates the mechanical construction of the distribution system. Our novel approach combines the division of the light intensity and its steering in one element, called the front panel, which consists of a series of custom coated beamsplitters that have different reflectivity values. The incoming light pulse is simultaneously divided and steered into the system with the final result being an array of light beams propagating towards the detector segments. The size of each segment, optimised for the Muon g-2 experiment, is 2.5×2.5 cm^2 with a total of 54 segments at each station. An example of a distribution system with an output matrix of 9×6 can be seen in Fig. 2. Outgoing beams are labeled G_{rc}, where r and c stands for row and column number, respectively.

Moreover, a minimum material thickness is present in the path of particles to the detector. The total thickness of glass found in the particle's path is 5 mm, which includes 2 mm thick beamsplitters

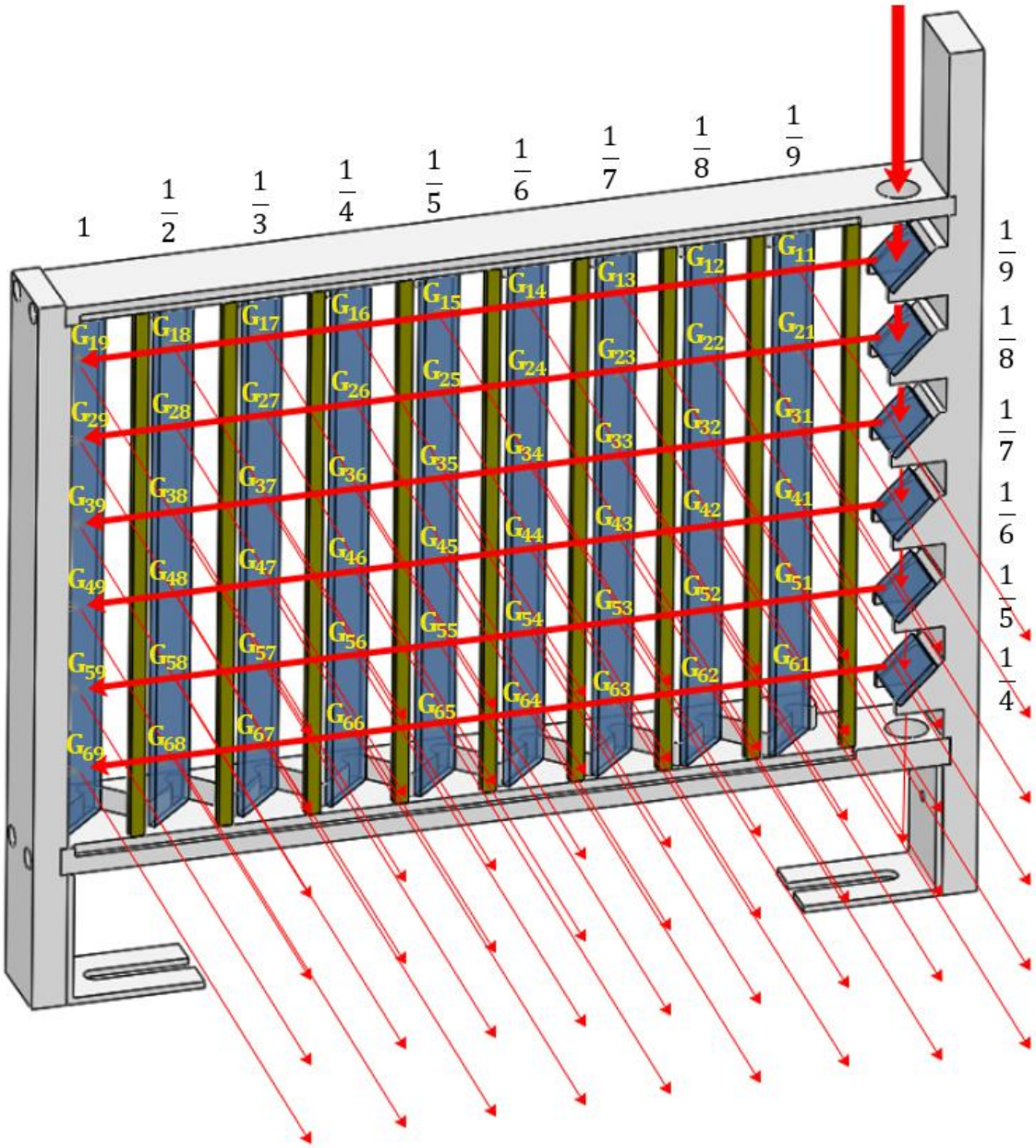

Figure 2. The schematic drawing of the frame named Pisa - Trieste (PiTs) after INFN Sections responsible for its development, with light path and ideal beam splitter reflectances is shown. The beam splitters are made of a single glass piece and have anti-reflective coating on one side and the specified reflective coating on the other side. The final version would have the fractions rounded to integer percent values. Although reflection coatings with more decimal numbers can be ordered, the cost scales up thus the lowest acceptable precision was chosen.

at 45° and the 2 mm thick ground glass diffuser in front of the detectors. This is important since we want to minimise the energy loss of incoming particles (i.e. interaction with light distribution system) during their propagation to the detectors. The average, over various types of glass, radiation length is about 12 cm which is big enough to minimize the impact on positrons propagating through

it. The front panel apparatus is scalable in the case where a large number of calibration channels are involved. The vertical beamsplitters are glued to previously prepared supports at $45° \pm 1°$ with respect to the normal of the front panel. This guarantees mechanical stability while alignment of the optical elements is provided by the machining precision. One potential complication in using such a system is that the reflectances from a surface are polarisation dependent and care must be taken to chose either the right input polarisation or depolarise the light beam before entering the panel. There is an additional light exit at the bottom of the panel that is used for monitoring the light source, which is either a laser directly coupled to the frame or a laser light coming through an optical fibre to the station. The light coming out at the bottom of the panel is proportional to each of the outgoing light matrix elements in the front panel.

2.1 Output beam matrix photon statistics

In the classical description, a beamsplitter splits the intensity of the input beam into two output beams whose intensities depend on the beam splitter transmitivity (or reflectivity). On the other hand, the quantum mechanical behaviour of a beam splitter is described by the probability to transmit (or reflect) a photon [12]. In fact, behaviour of an ideal lossless beamsplitter can be described as a binary selector that randomly transmits or reflects incoming photons one by one. We simulated our distribution system using random number generators (0 to 1) where photons are selected according to the condition imposed by the beamsplitter transmittance, T. If the randomly generated number is greater than T, an incoming photon is transmitted, else it is reflected. The number of loop iterations is equal to the number of photons coming to the beamsplitter. This process is repeated for every beamsplitter in the light distribution system.

At the end of this process, there should be 2000 photons in each channel. The requirement comes from the energy threshold in the Muon g-2 T-method analysis [13], which is about 2 GeV. We find that about 1000 photons/GeV are produced in the crystals [14], thus 2000 photons in every element of the output matrix are needed. If we use the beamsplitter reflectances from Fig. 2, $N_{in} = 162000$ photons will give the desired number of photons in the output matrix. This number was used as the input parameter in our Monte Carlo simulation where N_{in} photons at the front panel entrance encounter a beamsplitter with an $\frac{1}{9}$ reflectance. It follows that every ninth photon is reflected, and the number of reflected photons is used at the input of the second stage, which also consists of a beamsplitter with $\frac{1}{9}$ reflectivity. The transmitted light output is passed to a second random number generator that represents a $\frac{1}{8}$ beamsplitter. The interaction of the photons with a beamsplitter is considered to be lossless. This procedure is repeated until all the output matrix elements, plus the calibration output, are calculated according to the light path and reflectances shown in Fig. 2.

The simulation was verified by matching the N_{in} photons present at the input to the sum of the output matrix and monitoring port. The errors on photon numbers in each of the output matrix elements are the result of 10^4 simulations. The standard deviation in each matrix element is equal to the $\sqrt{N_{rc}}$, where N_{rc} is a number of photons in r-th row and c-th column of the front panel (see Fig. 2), as expected and does not depend on the photon propagation path. The relative error is 2.5%.

It is important to mention that all 54 calibration pulses do not fall onto the detectors at the same time since each beam inside the front panel propagates along a different optical path. The

optical path lengths of the different output matrix elements have been determined from Fig. 2, while taking into account the propagation through the beamsplitter material whose index of refraction value $n = 1.52$ was separately measured. The time delay information can be easily accounted for since it is determined by the geometry of the front panel. Although the maximum delay is on the order of a nanosecond, it can still be used for timing purposes since the delay for each channel can be easily calculated.

3 Front panel tests

The light distribution front panel was tested for mechanical stability, alignment precision, light intensity distribution stability and distribution precision.

3.1 Alignment precision and mechanical stability

Beamsplitters of a single reflectivity, namely commercially available soda lime window glass, were used in order to lower the costs of the prototype construction. Their index of refraction was obtained by means of Fresnel equations. The reflectance for unpolarized light was calculated from the value of the index of refraction and its value at 45° is $(4.1 \pm 0.2)\%$. As a consequence of using low quality glass, different elements of the outgoing light matrix have different intensities which differ from the calculated ones up to 25%. However, the alignment precision can be measured, and it can be inferred from a setup shown in Fig. 3 where the white paper is placed at the supposed position of the front face of the Cherenkov crystals.

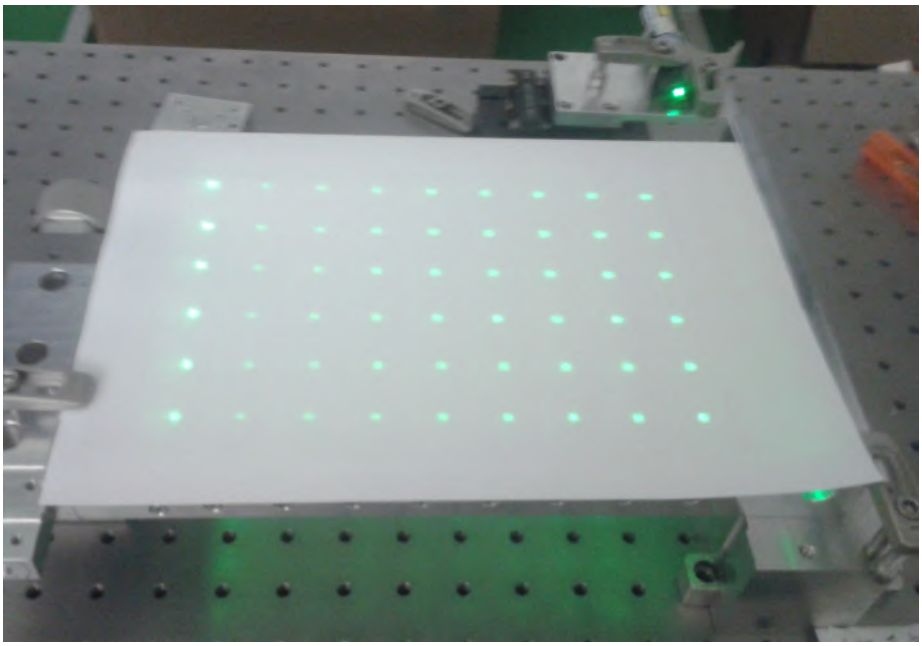

Figure 3. Picture of the 6×9 light matrix. The green laser light is entering the matrix from the top right corner. All the beam splitters have the same reflectivity. A white paper is put in front of the panel for display purposes.

The light source (Innolight Prometheus laser) was coupled to the front panel through a fibre with a numerical aperture NA = 0.22 whose output was connected to a Thorlabs SMA collimator with numerical aperture NA = 0.57 and focal length f = 4.34 mm. Measurements with a CCD camera of the beam profile after the collimator have shown that the beam has a diameter of 3.8 mm after 40 cm of propagation, which is the maximum path length through the panel.

The alignment of the outgoing light matrix was also checked by observing the light matrix elements' distribution at a distance of 2.5 m, which is more than one order of magnitude farther away than the detector's distance from the front panel in the Muon g-2 experiment. The maximum

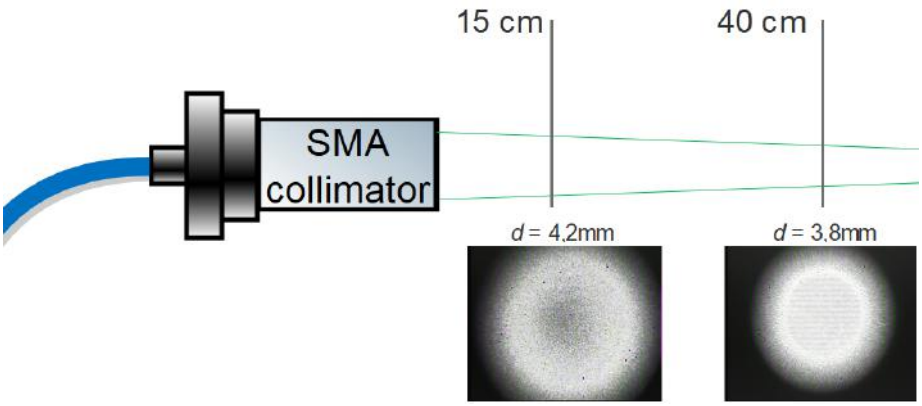

Figure 4. Beam profiles at 15 and 40 cm distance from the collimator, respectively.

deviation of each matrix point from the expected position was 6 cm. The expected detector's distance is 14 cm, which makes the projected maximum deviation smaller than 3.5 mm. This value is well within the crystal area $A = 2.5 \times 2.5\ cm^2$. Even if the detector active area is considered $A = 1.2 \times 1.2\ cm^2$, the beam would fall on it. However, before entering the crystal, the beam is diffused to guarantee the coverage of the entire active area even if it is not centred with respect to the longitudinal crystal axis. The deviation can be further minimised by a careful alignment of the beamsplitters but this might be an issue in the case of large scale production.

The next test regards the pointing stability, which was measured with a setup shown in Fig. 5.

The alignment stability was measured by placing two position sensitive photodiodes (Newport Conex-PSD9) at a distance of 15 cm from the front panel. The intensity of the laser beam as well as its vertical and horizontal position were recorded. The measurement period lasted about 2.5 hours and data were taken with a CW laser source at $\lambda = 532$ nm for two different output matrix elements with the longest optical paths, i.e. the 5th and 6th mirror in the last column of the panel. The measurements were taken simultaneously. The results can be seen in Fig. 6 and they are within the tolerances of the system given by the dimensions of the crystals.

The plots were obtained by calculating the weighted centre of distribution before plotting the relative distance to each of the measured points in the

3.2 Light distribution

The stability of the light distribution has been evaluated with the same setup shown in Fig. 5. In the Fig. 7 the ratio of two output light matrix elements can be seen for a period of about 3 hours. The next step in the characterisation and validation of the front panel is the measurement of the intensity of various elements in the light output matrix. For this purpose, two elements from the output matrix with an equal number of reflections were chosen since the expected power is equal for these two elements. A pulsed laser (Alphalas Picopower LD-405-10) at $\lambda = 405$ nm, with $t \approx 1$ ns, was used as a source, since it reproduces the characteristics of the expected signal (wavelength, luminous energy, pulse shape and pulse repetition [3]). The results are shown in Table 3.2. The measurements were taken with a commercial power meter.

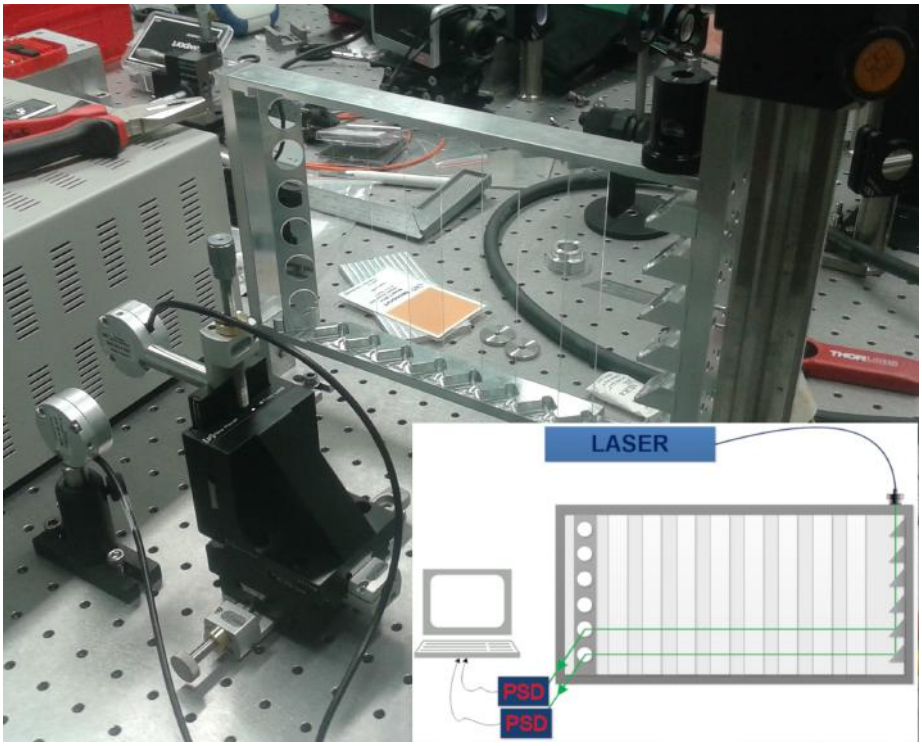

Figure 5. Picture of the setup for alignment stability checking. The front panel and two position sensitive diodes can be seen.

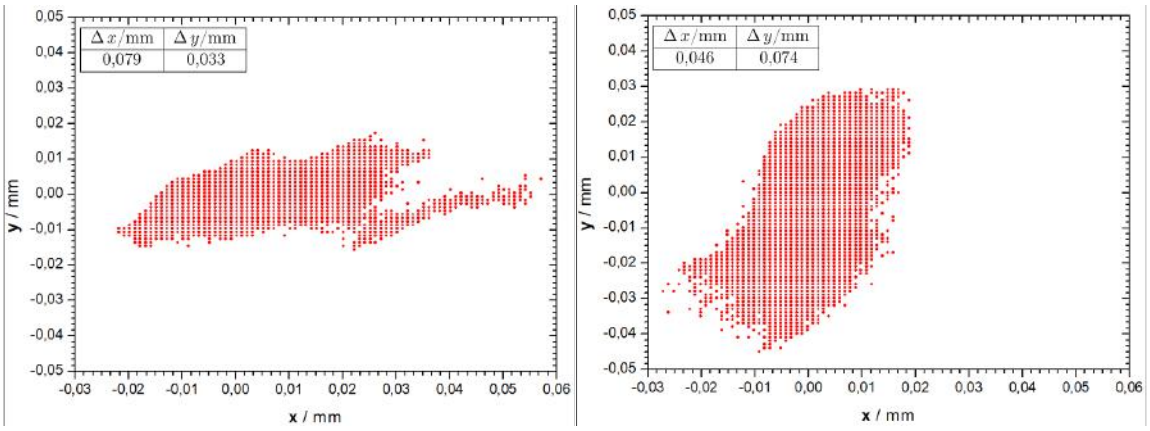

Figure 6. Results of the alignment stability measurement. The origin is determined by the weighted centre of distribution. The maximum excursion for both output matrix elements is lower than 0.1 mm in x and y directions.

The obtained results were compared with the ones obtained by simulation described in Section 2.1 where a random value up to a ±20% on beamsplitter reflectance was added to the nominal one. The results are shown in Fig. 8. The error on reflactance value was greatly exaggerated for display purposes (see Fig. 8) and is an order of magnitude higher than one expected from the manufacturer's specifications.

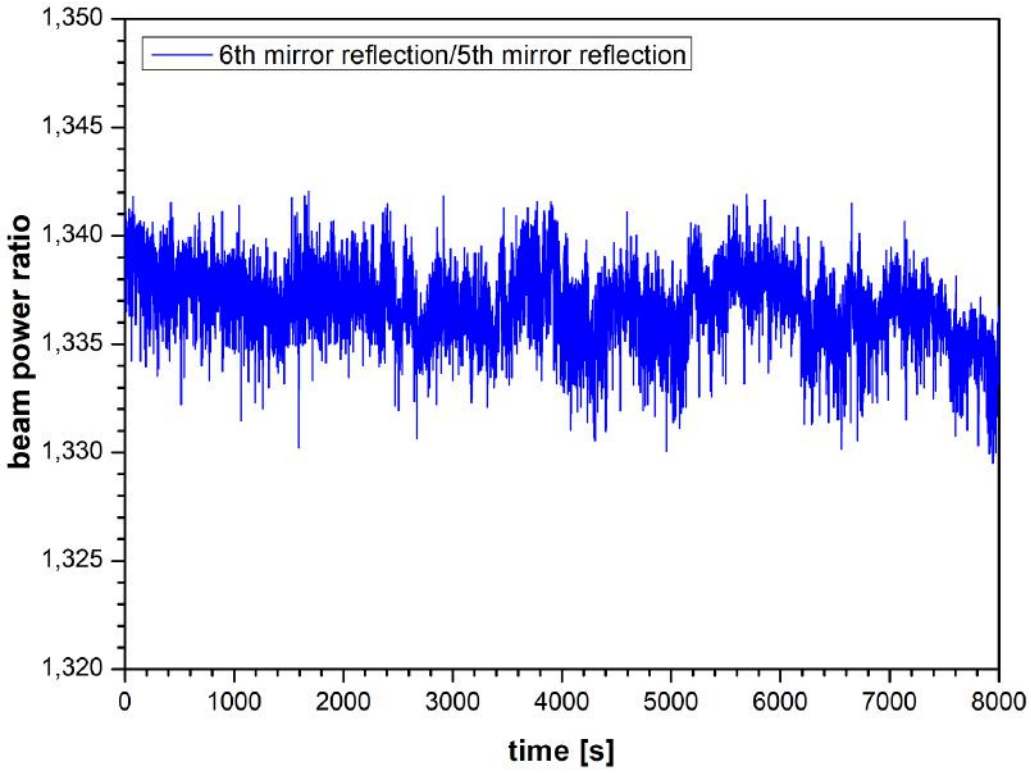

Figure 7. Ratio of light intensity in two of the light matrix outputs. The deviation from the constant value can be attributed to changing offset values in the two detectors. However the deviation is at per mill level which is within the tolerances of the experiment.

matrix element	expected power / nW	power / nW
G_{12}	56	59
G_{21}	56	53
G_{22}	50	53
G_{31}	50	48

Table 1. The expected vs measured power. The intensity ratio between the output matrix elements with the same history is $G_{21}/G_{12} = 1.116$ and $G_{22}/G_{13} = 1.114$. The uncertainty of the measurement is 5 % according to the detector specification (Thorlabs PM160).

3.3 Light diffusion

Since uniform illumination of the sensor is one of the main calibration requirements, the output beam profile from a fibre was studied in order to select a collimating system that will give the maximum beam dimensions with minimum light loss during propagation to the detector. A single ground glass diffuser was chosen, which covers the entire front panel area and provides uniform illumination of the detector. A white cardboard tube ($25 \times 25 \times 140$ mm^3) is used to simulate the crystal geometry in a single calorimeter segment, which can be seen in Fig. 9. The choice of the white cardboard was made considering that one of the possibile calorimeter crystal wrappings was

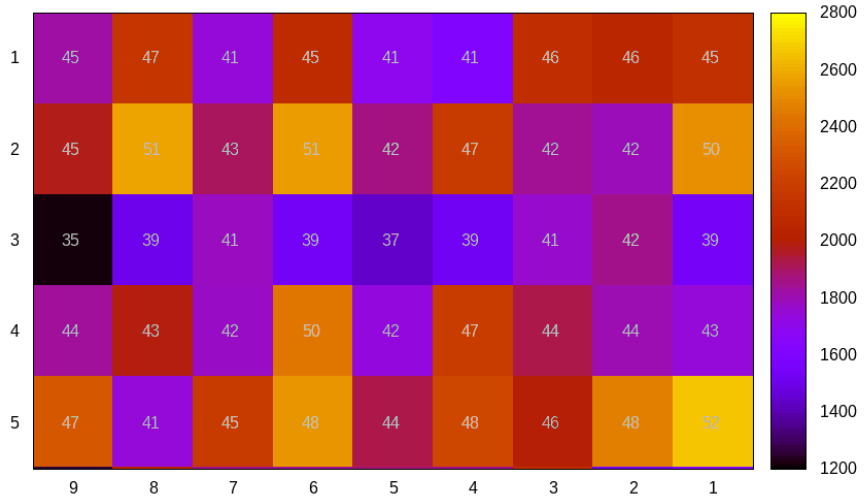

Figure 8. Average number of photons in colorcode and standard deviation in gray numbers on front panel output 9×6 matrix with $N_{in} = 162000$ photons at the input.

a white Millipore. However black Tedlar was chosen for the actual experiment. The light intensity exiting the cardboard tube was measured with an exposed CCD, from a Canon EOS 6D camera, placed at the other end of the tube. Beam cross section is digitally captured and the intensity profile is obtained. The profile is created from the integration of multiple pulses since the camera used is insensitive to a single pulse.

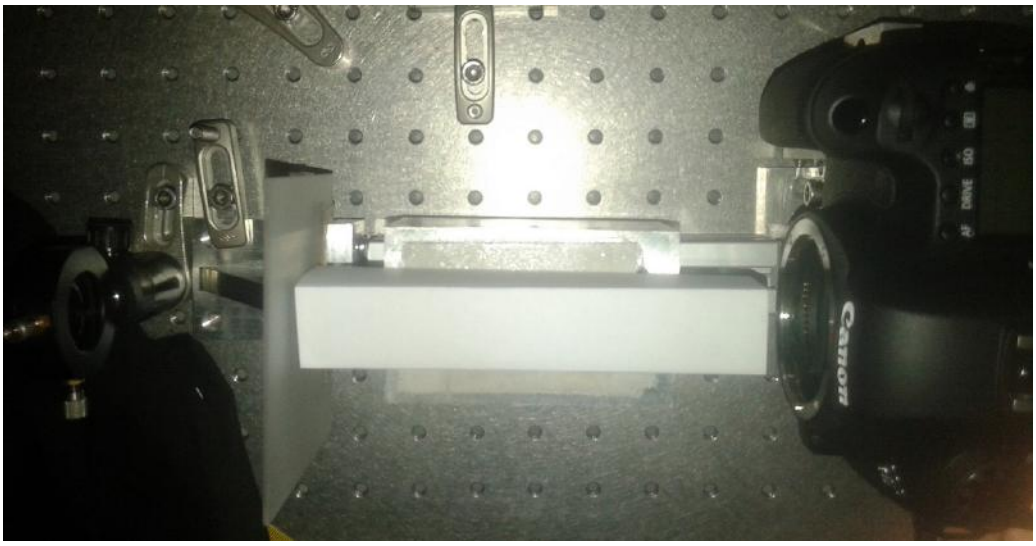

Figure 9. Illumination of the sensor after the distribution panel and diffuser setup.

The intensity variation across the crystal is shown in Fig. 10. The Actual SiPM size is indicated by a black square. The shadow on the top is caused by the limited sensor size nad the actual enclosure. If we focus on the part of the intensity corresponding to a detector size relevant for our experiment, we can see that the intensity variation across the detector surface is less than 10%.

Since the actual value of the signal is obtained by summing the signal in single pixels this does not represent a problem for the experiment.

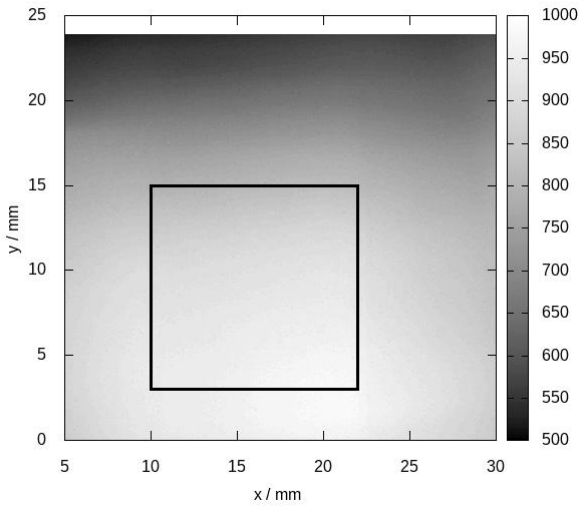

Figure 10. Intensity heatmap showing the crystal size 25 x 25 mm^2. The SiPM in the Muon $g-2$ experiment is indicated by a black square with the surface area of 12 x 12 mm^2. The position of the SiPM on the crystal face may vary in the actual experiment. The measurement has been done simulating the wrapped crystal with a paper tube of the same dimensions.

4 Conclusion

A new light distribution method is presented in this work and its feasibility is demonstrated. The stability of the system is within the experiment's requirements. The advantages over the conventional approach include the economic use of laser light, direct monitoring of light intensity and easily deducible time delay of the light pulses. Furthermore, in this system, the light losses are minimal, which relaxes the requirements on the light source and avoids potential security issues while guaranteeing stability of the light distribution. However, the conventional approach based on diffusers and fibers was chosen for the Muon g-2 experiment due to limited time available to test the prototype presented in this work.

Acknowledgments

We thank Fabrizio Scuri and Stefano Veronesi for the fruitful discussions in the early stage of the experiment. This research was supported by Instituto Nazionale di Fisica Nucleare (Italy), by Fermi Research Alliance, LLC under Contract No. DE-AC02-07CH11359 with the United States Department of Energy, and by the EU Horizon 2020 Research and Innovation Program under the Marie Sklodowska-Curie Grant Agreement No.690835 and No.734303. This work was also partially supported by EU projects No. KK.01.1.1.01.0001 and RC.2.2.06.-0001: Research

Infrastructure for Campus-based Laboratories at the University of Rijeka. The authors also wish to express their gratitude to the mechanical workshop of the INFN Sezione di Trieste where the prototype distribution panel was constructed.

References

[1] M. C. van Woerden,*"Upgrade of the Laser calibration system for the ATLAS hadronic calorimeter TileCal", Nuclear Instruments and Methods in Physics Research A: Accelerators, Spectrometers, Detectors and Associated Equipment, 824, pg. 64–66 (2016).*

[2] M. Anfreville et al.,*"Laser monitoring system for the CMS lead tungstate crystal calorimeter", Nuclear Instruments and Methods in Physics Research Section A: Accelerators, Spectrometers, Detectors and Associated Equipment, 292 pg. 594 (2008).*

[3] A. Anastasi et al.,*"Test of candidate light distributors for the muon (g-2) laser calibration system", Nuclear Instruments and Methods in Physics Research Section A: Accelerators, Spectrometers, Detectors and Associated Equipment, 788 pg. 43 (2015).*

[4] Y. Zhang, J. Liu, M. Xiao, F. Zhanga and T. Zhang,*"Laser calibration system in JUNO", Journal of Instrumentation, Vol. 14 (2019).*

[5] J. Grange et al.,"Muon (g-2) Technical Design Report" (2015), URL

[6] G.T. Danby et al., *"The Brookhaven muon storage ring magnet", Nuclear Instruments and Methods in Physics Research Section A: Accelerators, Spectrometers, Detectors and Associated Equipment, 457, 151 - 174 (2001)*

[7] L.P. Alonzi et al., *"The calorimeter system of the new muon g-2 experiment at Fermilab", Nuclear Instruments and Methods in Physics Research Section A: Accelerators, Spectrometers, Detectors and Associated Equipment, 824, pg. 718-720 (2016)*

[8] A. Anastasi et al., *The laser-based gain monitoring system of the calorimeters in the Muon g-2 experiment at Fermilab, Journal of Instrumentation, 14, 11025, (2019)*

[9] J. Sakai, T. Kimura,*"Bending loss of propagation modes in arbitrary-index profile optical fibers", Applied Optics Vol. 17, 10, pg. 1499–1506 (1978).*

[10] A. Argyros, R. Lwin, M. C.J. Large,*"Bend loss in highly multimode fibres", Optics Express Vol. 16, 23, pg. 18590-18598 (2008).*

[11] A. Anastasi et al.,*"The calibration system of the new g-2 experiment at Fermilab", Nuclear Instruments and Methods in Physics Research Section A: Accelerators, Spectrometers, Detectors and Associated Equipment, 824 pg. 716 (2016).*

[12] C. H. Holbrow, E. Galvez, and M. E. Parks,*"Photon quantum mechanics and beam splitters ", American Journal of Physics, 70 pg. 260 (2002).*

[13] G. W. Bennet et al.*"Final report of the E821 muon anomalous magnetic moment measurement at BNL", Phys. Rev. D 73, pg. 072003 (2006)*

[14] A. Anastasi et al.,*"Electron beam test of key elements of the laser-based calibration system for the Muon g-2 experiment", Nuclear Instruments and Methods in Physics Research Section A: Accelerators, Spectrometers, Detectors and Associated Equipment, 842 pg. 86 (2017).*